International Journal of Refrigeration 116 (2020) 59–69

Contents lists available at ScienceDirect

International Journal of Refrigeration

journal homepage: www.elsevier.com/locate/ijrefrig

Integrated CO_2 system with HVAC and hot water for hotels: Field measurements and performance evaluation

S. Smitt*, I. Tolstorebrov, A. Hafner

Norwegian University of Science and Technology, Kolbjørn Hejes vei 1D, Trondheim 7491, Norway

ARTICLE INFO

Article history:
Received 13 December 2019
Revised 20 March 2020
Accepted 23 March 2020
Available online 8 April 2020

Keywords:
R744
Heat pump
HVAC
Hot water
Thermal storage
Hotel energy systems

ABSTRACT

This study investigates the performance of an integrated CO_2 (R744) heat pump and chiller unit in a Norwegian hotel. The system consists of a single unit for heating, cooling and hot water with an integrated thermal storage. The thermal system of the hotel is described and data from the first year of operation are analyzed. Using the field measurements, hot water loads and COPs are calculated and averaged to 20-minute intervals. The heating and cooling capacities supplied by the R744 unit are studied on a weekly and monthly basis to evaluate the seasonal behavior of the system. The hot water storage holds an energy capacity of 350 kWh at fully charged conditions and demonstrates peak demand reductions of more than 100 kW during a 2-day period. The results show that the hot water usage accounts for 52% of the annual heat load of the hotel. Energy efficiency analysis of the integrated R744 system reveals an annual system SCOP of 2.90, and thus an untapped system potential that can be exploited by increasing the AC load delivered by the R744 unit. Other factors that greatly influence the efficiency of the system are variations in the ambient temperature and high gas cooler exit temperatures. The latter is often a result of high temperatures in the water returning from the subsystems of the hotel. This can be improved by reducing the number of starts and stops of the R744 unit and by insuring stratification in hot water tanks.

Système de CVC et de production d'eau chaude intégré au CO_2 pour les hôtels : mesures sur le terrain et évaluation des performances

Mots-clés: R744; Pompe à chaleur ; CVC; Eau chaude; Stockage de chaleur; Systèmes énergétiques dans l'hôtellerie

1. Introduction

In order to secure a sustainable future, it is necessary to adopt more efficient means of converting, storing and using thermal energy. Buildings are directly responsible for more than 40% of end-use energy consumption and CO_2 emissions in the EU (EC, 2010). Non-residential buildings, which are largely represented by the commercial sector, account for 35% of the energy use and related emissions (Eurostat, 2017). The potential energy savings within the commercial sector is estimated to 30%, which can be achieved by implementing measures to manage demand and increase energy efficiency (Economidou et al., 2011; EC, 2006). Hotels are categorized as high energy demanding buildings, due to their operational characteristics and the behavior of occupants (HES, 2011). The application of conventional thermal energy sources in hotels is extensive, such as fossil fuels and electric boilers for heating in large inefficient central systems (Dalton et al., 2008). Excessive use of electrical power by peak heating and the use of low-efficiency air-conditioning (AC) units aggravate the electricity problems society is facing. Existing hotels exhibit the most severe problems of excessively high energy demand rates, inevitably requiring renovations along with retrofitting of thermal systems (Santamouris et al., 1996).

Vapor compression systems are among the most energy-efficient methods of providing heating and cooling in buildings (Liu et al., 2017). An increased focus on environmentally friendly

* Corresponding author.
E-mail addresses: silje.smitt@ntnu.no (S. Smitt), ignat.tolstorebrov@ntnu.no (I. Tolstorebrov), armin.hafner@ntnu.no (A. Hafner).

https://doi.org/10.1016/j.ijrefrig.2020.03.021

Nomenclature

COP	Coefficient of Performance
DHW	Domestic Hot Water
SH	Space heating
T	Temperature [°C]
V	volume [l]
C_p	specific heat capacity [kWh kg^{-1} K^{-1}]
ref	reference
i	time step index
set	setpoint
E	Energy [kWh]
AC	Air Conditioning
F.S.	Full Scale
$\dot{Q}$	cooling or heating load [kW]
$\dot{m}$	mass flow rate [kg s^{-1}]
$\dot{W}$	power [kW]
P	Pressure [bar]
HPWH	Heat Pump Water Heater
comp	compressors
fans	evaporator fans
pumps	all system pumps
aux, el	auxiliary electrical systems
evap	evaporation
w	supply water
exit	exit
gc	gas cooler
a	ambient
avg	average
SH	space heating
DHW	Domestic Hot Water
AC	Air conditioning
sys	system
min	minimum
max	maximum
ch	DHW charging
nch	No DHW charging
HVAC	Heating, Ventilation, and Air-Conditioning
usage	consumption by end users
supply	supply by heat pump
HFC	Hydrofluorocarbon

Greek symbols

Δ	change
ρ	density [kg m^{-3}]

solutions together with a global effort to reduce the application of fluorinated gases is strengthening the position of natural refrigerants (UNEP, 2016; EP and EC, 2014). Carbon dioxide (R744) is a natural refrigerant with negligible environmental impact and favorable thermodynamic properties (Lorentzen, 1994; Gullo et al., 2019; Ciconkov, 2018). It is inexpensive, readily available and is neither flammable nor toxic. These qualities make R744 suitable in applications where other natural refrigerants, such as ammonia and propane, are challenging due to safety concerns (Bolaji and Huan, 2013). R744 is firmly established in both heating and refrigeration applications and is accepted as a viable alternative in several sectors, e.g. supermarket, transportation, domestic hot water (DHW) heat pumps and industrial processes (Gullo et al., 2018; Hafner, 2015; Nekså et al., 2010). The distinctive temperature glide of R744 in the gas cooler during transcritical operations allows for efficient heating of water (Nekså, 2002; Nekså et al., 1998), even up to temperatures of 90 °C (Bamigbetan et al., 2017). In the Japanese market alone, more than 5 million R744 heat pump water heaters (HPWHs) are installed (Shecco, 2016). However, as illustrated by Cecchinato et al. (2005), a suitable R744 heat pump design is imperative to ensure a high efficiency when compared with hydrofluorocarbon (HFC) installations, such as R134a. In their later work, Cecchinato et al. (2010) identified compressor capacity rate and secondary fluid temperatures as key influencing factors on optimum R744 high pressure, and thus cycle efficiency. Minetto (2011) presented experimental results from the development of an R744 air/water HPWH for residential buildings, and also concluded that optimum operating high-pressure conditions are highly dependent on both inlet temperature and production setpoint temperature for hot water. Several other works have tackled the high-pressure control problem to achieve maximum cycle coefficient of performance (COP) (Yang et al., 2015; Hu et al., 2015; Wang et al., 2013; Cecchinato et al., 2012). The design and operation of the secondary system, especially the DHW storage, is equally important to ensure high efficiency in R744 HPWH installations. It is firmly established that reducing the return temperature from the secondary system to the gas cooler will limit the R744 gas cooler outlet temperature, and thus enhance cycle COP (Lorentzen, 1994). Thermal stratification of the DHW storage should therefore be employed to reduce mixing and ensure the return of cold water to the gas cooler (Fernandez et al., 2010). The impact of the return temperature of water on cycle efficiency, with respect to ambient air and city water temperatures, was illustrated by Yokoyama et al. (2007). They concluded that the R744 HPWH efficiency does not always increase with ambient temperature, as the storage efficiency decreases with the increase of city water temperatures. Besides DHW, another application of the transcritical R744 heat pump is a combined heat supply system for space heating (SH) and DHW by the means of several gas coolers in series (Stene, 2005; Heinz et al., 2010).

R744 systems have a long tradition in refrigeration processes. In the European supermarket sector alone, more than 16,000 stores are relying on R744, where 14% of the installations are operating in the transcritical region (Skačanová and De Oña, 2019). Transcritical R744 systems with integrated heating and cooling applications are traditionally found within this sector, where excess heat is recovered as a byproduct of the refrigeration process (Pardiñas et al., 2018; Hafner, 2017; Girotto, 2016). Combined operations with heat recovery highly enhance the performance of the R744 refrigeration system (Karampour and Sawalha, 2017), and can be especially beneficial in warm climate applications, as demonstrated by Gullo (2019). However, the control strategy during these operations of heating and cooling can highly influence the efficiency (Sarkar et al., 2004; Sarkar et al., 2006). Water storage units can be applied to compensate for asynchronous heating and cooling demands, and reduce peak load operation (D'Agaro et al., 2019; Polzot et al., 2016). Integrated heating, ventilation, air-conditioning (HVAC) and DHW systems for buildings are widely applied (Fabrizio et al., 2014; Chua et al., 2010; Omer, 2008). However, applications of R744 integrated HVAC and DHW systems outside the supermarket sector are not well-established nor sufficiently documented. The current status of R744 systems proves the potential benefits of implementing integrated R744 in buildings with large DHW demands, such as hotels. Byrne et al. (2009) conducted a theoretical comparison between an integrated R744 unit for HVAC and DHW with a state-of-the-art R407A system, and found the energy performances comparable. Minetto et al. (2016) presented a water-side reversible R744 HVAC and DHW unit that operated highly efficient during DHW production. However, COP was significantly reduced during the SH heating mode, due to high return temperatures from the heating system. Tosato et al. (2019) presented a layout of an integrated HVAC and DHW R744 unit for a hotel located in Northern Italy, where ground-water was utilized as a heat source. Results from a charging cycle of the 1.5 m^3 DHW storage revealed a COP of 4.1 during the process. As of yet, no studies have been con-

duction of long term operations of R744 systems in hotels. At the same time, there is a need to evaluate these systems with respect to DHW storage capacities during different operational modes, e.g. charging and discharging. This paper presents the evaluation of long-term logged data from an integrated R744 unit installed in a hotel in Norway. A 6 m^3 DHW storage is included in the thermal system for peak load shaving, the operation of which is presented and discussed.

2. System description

The R744 system analyzed in this work is part of the existing heating system for a medium-size hotel in Værnes, Norway. The system provides HVAC and DHW for a floor area of approximately 9000 m^2, which includes 157 guest rooms. The hotel was built in 1987, with an annual heat energy demand of approximately 1.2 GWh prior to the refurbishment of the thermal system in June 2018. The annual heat demand was reduced to approximately 1 GWh following the refurbishment. The location of the hotel is characterized by cold climate conditions with a normalized average annual temperature of 5.3 °C and 4276 heating degree days (HDD) (average from 1961 to 1990). HDD for the location of the hotel is calculated as described in Thom (1954) with Scandinavian standard values (Skaugen et al., 2002). The annual average temperature for the first year of operation was recorded to be 6.8 °C with 3860 HDD over the period from September 2018 to September 2019.

2.1. R744 heat pump and chiller unit

The previous thermal system of the hotel, consisting of an electric- and oil boiler, has been replaced with the R744 heat pump and chiller system. The first 6 months of operation revealed a monthly energy-saving potential of 59–69% (Smitt et al., 2019). The installed heating and AC cooling capacity is 280 kW and 75 kW, respectively. In this paper, *AC* is defined as the ventilation cooling load. Fig. 1 illustrates the configuration of the R744 heat pump and chiller unit and secondary distribution systems. The R744 unit is an adapted single-stage supermarket refrigeration unit with heat recovery towards two separate hydronic circuits. The compressor rack consists of four parallel compressors (displacement range from 17.8 to 21.2 $m^{-3}h^{-1}$ at 50 Hz). One compressor is equipped with a variable speed drive (VSD), while the three other compressors are controlled by ON/OFF. The compressors are activated based on the requested capacity. The VSD compressor is always active to meet the capacity setpoint between the constant capacity steps provided by the other compressors.

The main function of the R744 system is to provide heating and DHW for the hotel, which is achieved with the same strategy as for heat recovery in transcritical R744 supermarket units (Danfoss, 2015; Danfoss, 2012), with the exception that the heating load, rather than the cooling load, is the controlling parameter. The capacity control of the R744 unit is based on feedback signals from the hotel, such as from the DHW, ventilation- and radiator circuits. The building side supplies a heat demand signal to the R744 controller, which adjusts the setpoints for the compressor capacity and the high pressure. If an increase in capacity is requested, the setpoint for the evaporation temperature is temporarily reduced to activate another compressor in the rack. This somewhat unconventional control is due to the conversion of the R744 unit from a supermarket refrigeration rig. The high pressure P_{gc} is regulated based on the gas cooler outlet temperature $T_{gc,exit}$. The control principle of the gas cooler pressure is described in Gullo et al. (2016). The high pressure control valve (EV1) expands the fluid directly to the liquid separator at an intermediate pressure of 38–55 bar. Four air evaporators (50 kW at −15 °C) are fed from the liquid receiver. Thermostatic expansion valves (EV2–EV5) regulate the superheat at the exit of each evaporator. The number of active evaporators is dependent on the heating load. The gas returning from the evaporators is mixed with flash gas and is directed in a passage through the liquid receiver for heat exchange before compression. Also, a heat exchanger (HX) interface (75 kW at 12/7 °C) to the chilled water circuit (HX6) can be employed to recover heat if AC is needed. The chilled water produced by the R744 system is used to supplement the existing AC chiller unit, and is thus only applied as an auxiliary function during heat generation.

2.2. Subsystems and hot water storage

The system is designed to supply heat for ventilation heating, DHW and SH. Heat is supplied to the hydronic subsystems through two gas coolers in series, GC1 and GC2 as shown in Fig. 1, at high (> 60 °C) and medium (< 50 °C) temperatures. The medium temperature (MT) circuit provides heat primarily to ventilation batteries and a radiator/floor heating circuit. Remaining heat is used to preheat DHW through HX2 from approximately 8 to 30 °C. During winter operations, HX1 in the MT circuit is applied for defrosting of the evaporators through a brine circuit.

The high temperature (HT) circuit mainly supplies heat for DHW reheat through HX3. During operational conditions with negligible SH demand, the entirety of the DHW production can be covered with HX3. HX2 is then bypassed with valve MV1. Similarly, GC1 can be bypassed through the directional valve, DV1, if the DHW storage is fully charged and there is no demand for HT heat. The R744 unit will in these instances operate at a subcritical high-pressure level. The HT circuit also supplies extra heat thought HX5 for the radiators and floor heating during winter conditions. This is typically done when the setpoint temperature of the radiators exceeds the setpoint of the MT circuit. When the return temperature is higher than the setpoint temperature of the MT circuit, MV5 closes off the passage between MT and the radiators. A shunt circuit is then established exclusively between the radiators and HX5, to prevent an increase in water temperature to GC2.

The DHW subsystem consists of several tanks in series with a combined volume of 6 m^3. The subsystem is supplied with heat from the R744 unit through HX2 and HX3, or from the backup electric boiler through HX4. The system control is characterized by two distinctive modes of operation depending on the state of the DHW storage and whether active charging is needed. When active charging of the storage is unnecessary, the majority of the heating load is allocated to the MT circuit to cover the moderate temperature demands, e.g. radiators, floor and ventilation heating. Excess heat is allocated to the DHW subsystem, usually at a low load to meet the required DHW temperature.

The second mode of operation occurs during active charging of the DHW storage and is activated when the temperatures in tanks 1 or 3 fall below a threshold. A few steps are initiated to start the charging process. First, the setpoint of Pump P4 is changed to provide a higher flow rate. Then, the heat demand from the building is then given an offset signal to induce charging. The increase in demand triggers an increase in compressor load, which is maintained by temperature insurance of the HT and MT circuit supply temperatures. During the charging process, excess hot water is stored and moves through the series of tanks as the buffer is gradually charged from tank no. 1 to no. 10. Water is drawn from tank no. 10 and is sent through the heating process, in the same manner as described by Minetto (2011). The thermal storage is fully charged when the normally stratified storage reaches a high and uniform temperature. During discharge, water is drawn from tank no. 1 and is mixed in MV3 with cold water to a temperature of 55 °C before entering the supply line. The setpoint for DHW production is 66 °C. Once a week, the setpoint temperature is boosted to 86 °C, during which all tanks must meet the setpoint temperature for at

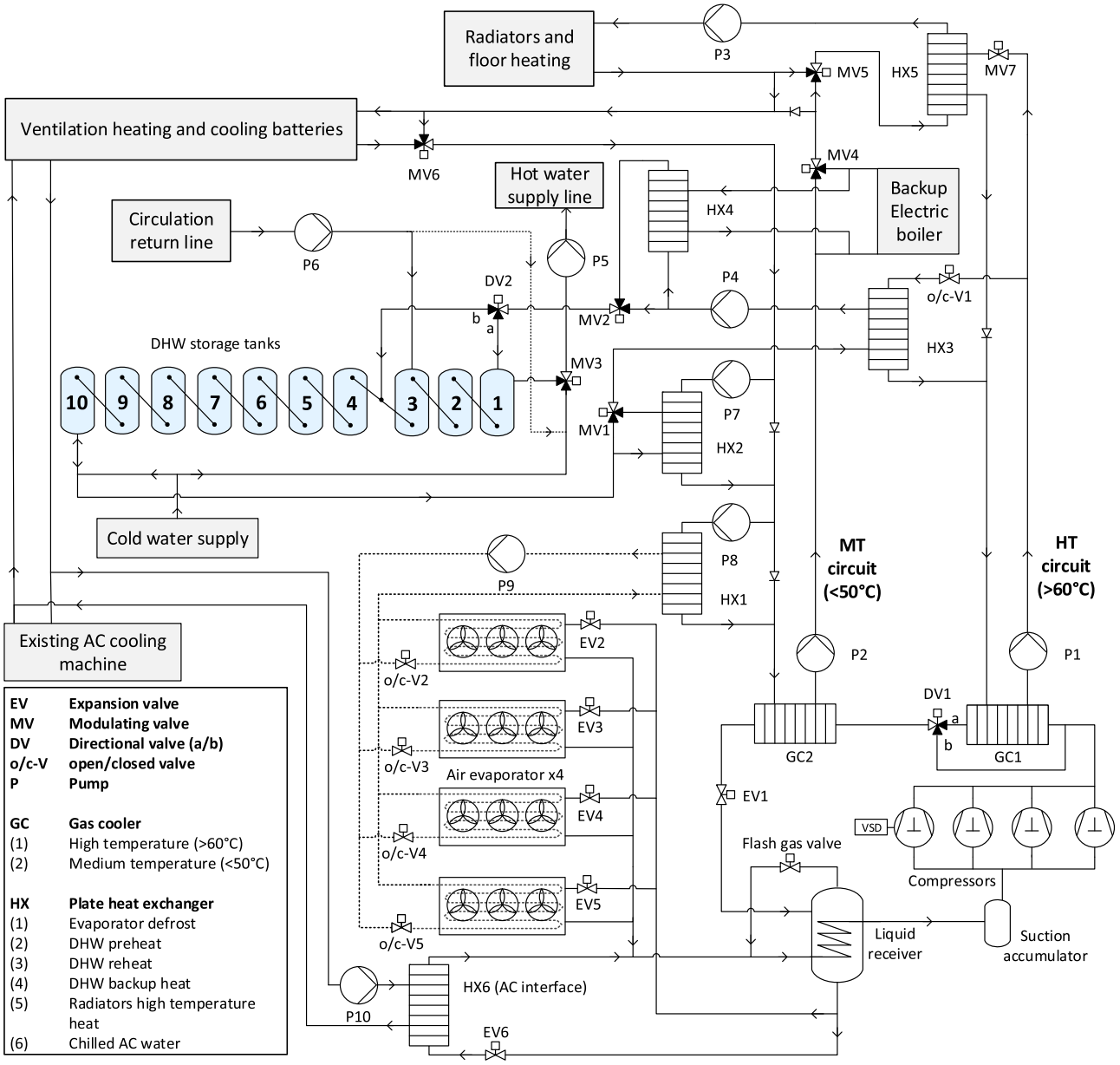

Fig. 1. Schematic drawing of the R744 heat pump and chiller unit with thermal storage and secondary system.

least one hour to prevent legionella growth. The start signal for the timer is reset if the temperature level has been reached. As additional insurance, heating elements are installed in each tank for temperature boosting purposes.

3. Data collection and evaluation methods

The secondary hydronic system is instrumented with temperature sensors (NTC10 thermistors, ± 0.2 K) and mass flow meters (oscillator mass flow sensor, class 2) in every fluid branch. Temperature sensors in the DHW tanks and secondary systems have been validated to operate within a range of ± 0.1 K. Heat flow meters for secondary fluids are installed at every HX (PT500 temperature sensors, oscillator mass flow sensor, class 2). Pressure sensors (± 0.3% at full scale), temperature sensors (PT500 temperature sensors, ± 0.15 + 0.002T) and electrical power supply monitors (energy analyzer in control unit, ± 2%) are installed in the R744 unit. The real-time field measurements of the hotel have been obtained via the web-monitoring software *IWMAC* (IWMAC, 2019). The measurements are updated continuously, but the data at a certain time is only logged by the measurement system if it differs from the value in the previous time step. The recorded data points are therefore regarded as constant step values within the specific time interval until the next recorded value. All the recorded data have been resampled and synchronized to the same time step, using the weighted average of the time intervals. The data used in this analysis were collected and processed for the period from September 2018 to September 2019.

3.1. Domestic hot water (DHW) loads

Due to the absence of an energy meter in the DHW supply line, the consumption load and mass flow rate are calculated using the energy balance equation on the DHW subsystem. The reference temperature, T_{ref}, represents the temperature of the cold supply water, which is fairly stable throughout the year. The water temperature is therefore assumed to keep a constant temperature of 8 °C. The energy stored in the tanks, E_{tanks} [kWh], at each time

step, *i*, is calculated by Eq. (1).

$$E_{tanks_i} = \rho V C_p \sum_{j=1}^{10} (T_{j_i} - T_{ref}) \quad (1)$$

where T_j is temperature measured in tank *j*, which holds a water volume, *V*, of 600 l. The temperature in the storage tanks normally varies between T_{ref} and 66 °C, and are measured in the middle of each tank, which gives a good overview of the temperature gradient across the storage. space Water density, ρ [kg m^{-3}], and specific heat capacity, C_p [kWh kg^{-1} K^{-1}], at the mean operation temperature of 30 °C are used in the calculations. Applying the energy balance on the DHW subsystem yields the following equation:

$$\frac{\Delta E_{tanks_i}}{dt_i} = \dot{Q}_{HX2_i} + \dot{Q}_{HX3_i} + \dot{Q}_{HX4_i} - \dot{Q}_{DHW_i} \quad (2)$$

where

$$\Delta E_{tanks_i} = E_{tanks_{i+1}} - E_{tanks_i} \quad (3)$$

$\dot{Q}_{DHW_i}$ [kW] in Eq. (2) is the heat load accompanying DHW usage. Other parameters are explained in Sections 2.1 and 2.2. Change of energy in the water storage at each time step, ΔE_{tanks_i} [kWh] (Eq. (3)), is defined as the difference between the current time step, *i*, and the next, $i+1$. The DHW heat load, (Eq. (4)), is derived from Eqs. (1) to (3). The heat losses from the storage tanks are accounted for in $\dot{Q}_{DHW_i}$. The average value of calculated measurement uncertainty [%] is presented in the equation.

$$\dot{Q}_{DHW_i} = \dot{Q}_{HX2_i} + \dot{Q}_{HX3_i} + \dot{Q}_{HX4_i} - \frac{\rho V C_p}{dt_i} \sum_{j=1}^{10} (T_{j_{i+1}} - T_{j_i}) \pm 4.5\% \quad (4)$$

The DHW consumption mass flow rate, $\dot{m}_{DHW_i}$ [kg s^{-1}], is then calculated as

$$\dot{m}_{DHW_i} = \frac{\dot{Q}_{DHW_i}}{(T_{set} - T_{ref}) C_p} \quad (5)$$

where T_{set} is the DHW supply setpoint temperature (55 °C).

3.2. Coefficients of performance (COPs)

Collected measurements for heating capacities, AC capacities and power consumption are used to calculated the COPs of the integrated thermal system. The total system COP [-], referred to as COP_{sys}, is defined as the ratio of useful thermal load to the total electricity consumption, using Eq. (6):

$$COP_{sys} = \frac{\dot{Q}_{GC1} + \dot{Q}_{GC2} + \dot{Q}_{AC}}{\dot{W}_{comp} + \dot{W}_{fans} + \dot{W}_{pumps} + \dot{W}_{aux,el}} \pm 6.2\% \quad (6)$$

where $\dot{W}_{comp}$, $\dot{W}_{fans}$ and $\dot{W}_{pumps}$ [kW] represent the combined electricity consumption for all compressors, evaporation fans and pumps, respectively. $\dot{W}_{aux,el}$ [kW] is the electricity consumption for auxiliary systems, such as control systems. $\dot{Q}_{AC}$ is the AC load that is supplied through HX6.

The heat pump COP, COP_h [-], is the ratio of the total heat load to the electricity necessary to provide the heating functions. This includes electricity consumption of the compressors and the fans in the evaporators, as shown in Eq. (7).

$$COP_h = \frac{\dot{Q}_{GC1} + \dot{Q}_{GC2}}{\dot{W}_{comp} + \dot{W}_{fans}} \pm 5.7\% \quad (7)$$

The COP of the AC chiller system is not evaluated as a singular parameter since cooling is not a controlling parameter in the R744 unit, but rather a byproduct of the heating operation.

The seasonal coefficient of performance (SCOP) for the entire heat pump system with/without boiler, $SCOP_{sys+el}$ [-] and $SCOP_{sys}$ [-], and SCOP for heating, $SCOP_h$ [-], are calculated as the ratio between supplied heating and/or AC cooling energy [kWh] to the work of compressors and auxiliary devices [kWh], as shown in Eqs. (8) and (9).

$$SCOP_{sys} = \frac{\sum(\int \dot{Q}_{GC1} + \int \dot{Q}_{GC2} + \int \dot{Q}_{AC})}{\sum(\int \dot{W}_{comp} + \int \dot{W}_{fans} + \int \dot{W}_{pumps} + \int \dot{W}_{aux,el})} \pm 6.2\% \quad (8)$$

$$SCOP_{sys+el} = \frac{\sum(\int \dot{Q}_{GC1} + \int \dot{Q}_{GC2} + \int \dot{Q}_{AC} + \int \dot{Q}_{EL})}{\sum(\int \dot{W}_{comp} + \int \dot{W}_{fans} + \int \dot{W}_{pumps} + \int \dot{W}_{aux,el} + \int \dot{W}_{EL})} \pm 10.5\% \quad (9)$$

$$SCOP_h = \frac{\sum(\int \dot{Q}_{GC1} + \int \dot{Q}_{GC2})}{\sum(\int \dot{W}_{comp} + \int \dot{W}_{fans})} \pm 5.7\% \quad (10)$$

where $\dot{Q}_{EL}$ and $\dot{W}_{EL}$ is the heat and power associated with the operation of the electric boiler, respectively.

4. System performance analysis

4.1. Analysis of key operating parameters

In order to assess the system performance during different operational conditions with variations in heating, DHW and AC loads, key operating parameters of the system are evaluated and discussed in this section. Specific periods are categorized based on weather conditions that demonstrate different seasonal performance of the system: summer (June through August), winter (November through March), and nominal for operating conditions representing fall and spring (September through October, April through May).

4.1.1. Key system operational parameters

Key R744 cycle parameters and high-side temperatures are analyzed. The studied parameters include ambient air temperature T_a [°C], R744 evaporation temperature T_{evap} [°C], as well as MT and HT supply water temperatures, represented by $T_{w,MT}$ and $T_{w,HT}$ [°C], respectively. The high pressure, P_{gc} [bar], and gas cooler outlet temperature, $T_{gc,exit}$ [°C] are included in the analysis. The performance of the system under four weeks of winter operation is shown in Fig. 2. The period is characterized by low ambient temperature and marginal AC loads.

As can be observed in Fig. 2, P_{gc} operates in the transcritical pressure region with a maximum working pressure of 100 bar. Relatively large fluctuations in pressure occur during this period, as a result of variations in $T_{gc,exit}$. Low fluid return temperature from the secondary thermal systems will consequently limit $T_{gc,exit}$ and thus also P_{gc}. However, some situations will cause unwanted high return temperatures from the MT circuit to the second gas cooler: (a) transitions between different modes of operation, (b) low load operations with many starts and stops, and (c) mixing in DHW tanks, which result in high return temperature during charging. The negative impact of high return temperature can be reduced by increasing the gas cooler pressure.

Heat is supplied to the secondary thermal system at the two different temperature levels $T_{w,MT}$ and $T_{w,HT}$. The MT and HT circuit setpoint temperatures are regulated based on outdoor temperature compensation curves, which varies from 25 to 50 °C and 60 to 70 °C, respectively. Fig. 2 shows that $T_{w,HT}$ generally operates between 65 and 70 °C.

The mass flows through the four air evaporators are controlled according to the superheat at the exit of each evaporator. Hence,

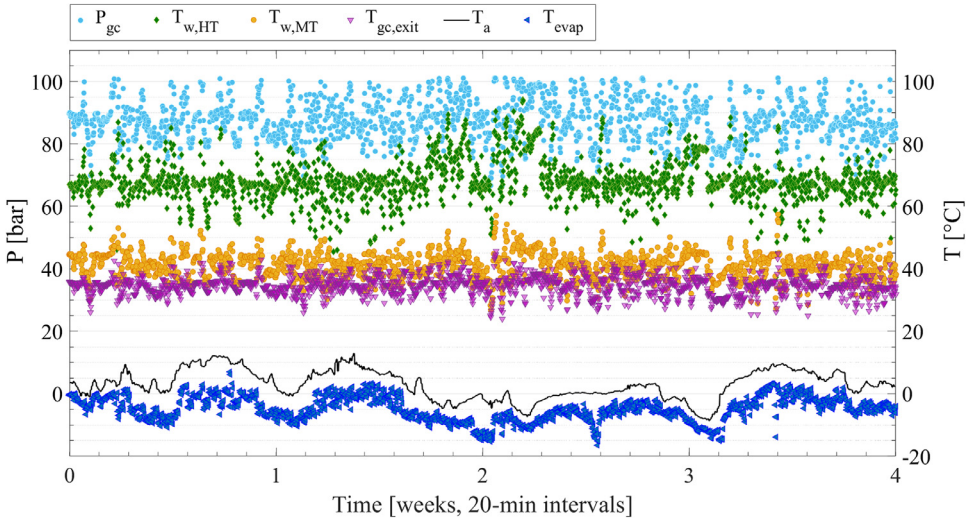

Fig. 2. Key operating parameters for winter operations (November 6th to December 4th 2018).

T_{evap} generally follows the pattern of T_a with a temperature difference determined by the superheat control. The setpoint for superheat is periodically changed according to temperature level of T_a. For the interval displayed in Fig. 2, the superheat setpoint is fixed to a minimum of 4 K. The sudden drop of T_{evap} is illustrated halfway through week 2. This behavior occurs when the heat load is increased, e.g. during heat pump start-up, capacity increase or during activation of additional evaporators. Hence, the setpoint of the evaporation, T_{evap}, is reduced to boost the discharge temperature and to increase the capacity. The reduction of T_{evap} is extra work for the compressors and cause excessive superheat that reduces COP considerably.

4.1.2. Domestic hot water (DHW) accumulation

The consumption of hot water typically follows a certain pattern dependent on the behavior of the residents and the operation of the hotel facilities. The major consumers of hot water in hotels are primarily guests, kitchens, laundry services and spa or pool facilities (Bohdanowicz, 2006; Lawson, 2001). Generally, the hot water consumption in hotel buildings is characterized by large consumption peaks for a few hours during the mornings and evenings (Ndoye and Sarr, 2008; Rankin and Rousseau, 2006; Deng and Burnett, 2002). In circumstances where no DHW storage buffer is installed, the high consumption peaks will be directly reflected in the hotel's power consumption. Fig. 3 shows the hot water average daily consumption profile, DHW_{usage} [kWh], and the profile of energy supplied by the heat pump to the storage, DHW_{supply} [kWh], over a period of one year. The average DHW daily usage during this period is 1104 kWh/day. However, significant variations in daily consumption were recorded with maximum and minimum values of 2480 and 480 kWh/day. On average, 2.3% of the DHW_{usage} is covered by the electric boiler.

As seen in Fig. 3, most of the DHW consumption occurs between hour 8 and midnight. The DHW usage during this time period accounts for 87% of the daily consumption. The activity level in the hotel is low between hours 0 and 6, hence the DHW usage is lower during this time. DHW_{usage} peaks occur during the hours 9 and 23 at values around 70 kWh. However, DHW_{supply} does not exceed 58 kWh due to the buffer effect granted by the storage, and demonstrates how the system handles power peaks on an average basis. The impact of the storage is the difference between DHW_{usage} and DHW_{supply}, which reaches a peak of 22 kWh during hour 8. The charging of the storage begins at hour 0 and declines to a minimum around hour 6, as the storage is fully charged. When

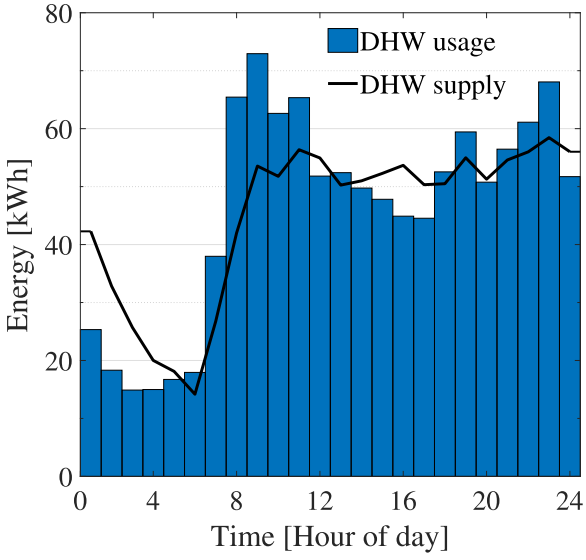

Fig. 3. Hourly-average DHW consumption and supply profiles over a one-year period.

DHW_{usage} increases to a peak of 73 kWh at hour 9, the storage is empty and active charging begins, holding a value between 50 and 55 kWh through the day.

The control strategy of the stratified heat storage in an R744 system is essential for successful operation, as described by Tammaro et al. (2016). Detailed operating parameters of the DHW storage are shown with a 20-minute resolution over a 2-day period in Fig. 4. Fig. 4A shows the temperature stratification across the storage, which is illustrated by the temperatures in tanks 1, 3, 5, 7 and 10, as labeled in Fig. 1. The storage load and the corresponding energy in the storage over the period are shown in Fig. 4B and C, respectively. The water temperature of the storage fluctuates between 8 and 78 °C during the period. The state of the storage can be determined by studying the temperatures *Tank*1 and *Tank*10. As the last tank in the series, *Tank*10 is sensitive to change in DHW mass flow rates entering and exiting the DHW subsystem. Supply water at 8 °C enters tank 10 during discharge and is gradually pushed through the storage as hot water is drawn from *Tank*1 and supplied to the hotel. The sudden drop in all temperatures in Fig. 4A illustrates the discharge of the storage

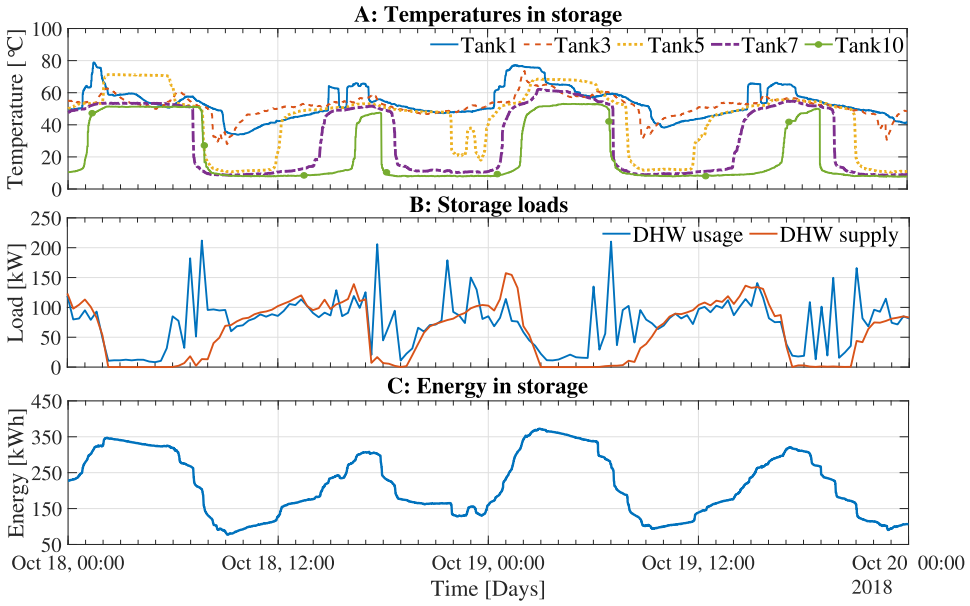

Fig. 4. Operation of the DHW subsystem over a 2-day period showing (a) storage temperature, (b) DHW usage and supply and (c) energy in the storage.

and corresponds to peaks in the *DHWusage*, as can be observed in Fig. 4B. The energy potential of the storage is fully exploited when *Tank*1 reaches its minimum water temperature. The charging of the storage is illustrated by the increase in the temperatures across the buffer. Hot water is supplied to the storage via tank 1 and is circulated through the buffer. The temperature boundary between hot and cold moves through the storage, as tank temperatures are lifted. As a consequence, the temperatures in the middle of the storage (tanks 3–7) can occasionally be higher than the temperature of tank 1 if the hot water supply temperature fluctuates during the charging process. This behavior is illustrated by *Tank5*, which sometimes is higher than *Tank1*. Simultaneously, cold water is drawn from tank 10 for heating, as explained in Section 2.2. The storage is charged when *Tank*10 reaches its peak temperature. As seen from Figs. 4A, there is a 24-hour pattern to the behavior of the DHW storage temperatures. The DHW storage energy is fully exerted and is recharged twice a day, which is in agreement with the findings in Fig. 3. Fig. 4B shows that the storage is typically charged for 7–10 h. The sudden drop in storage temperature can be seen in reference to the behavior of *DHWusage*. As shown in Fig. 4A and B, large *DHWusage* peaks in the range of 200 kW cause a rapid decrease in the storage temperatures. It can be observed from Fig. 4C that it takes approximately 2 hours to discharge the entire storage during these periods. There is still a high demand for DHW at hour 9 each day when the storage reaches its minimum energy potential. The hot water generated by the R744 unit is then supplied directly to the hotel to compensate for large demands. This system behavior indicates that the storage volume of 6 m^3 is not quite sufficient to meet the peak DHW demands of the hotel. This is especially evident in the mornings, as *Tank*1 drops below its setpoint of 55 °C. At fully charged conditions, the storage reaches an energy potential of approximately 350 kWh. A possible solution for the insufficient energy reserve in the storage is to store the water at higher temperatures. By increasing the water temperature in all tanks to 70 °C, one could increase the energy storage capacity with about 25%. Nevertheless, the storage buffer still provides a beneficial reduction of peak loads. This is represented by the difference between *DHWusage* and *DHWsupply*, which is more than 100 kW during peak hours. Another benefit of the large storage volume is higher flexibility in DHW production, which allows for low-intensity DHW generation over longer time intervals.

4.2. Evaluation of energy performance

The energy efficiency of the system including the provided heating, AC loads and COPs are evaluated in the following subsections.

4.2.1. Heating and AC cooling loads

Seasonal hourly-averaged heating and AC loads, $\dot{Q}$, of the integrated R744 system, together with hourly-averaged ambient temperatures, $T_{a,\ avg}$, and recorded maximum and minimum temperatures, $T_{a,max}$ and $T_{a,min}$, are shown in Fig. 5A–C. The specific load for DHW, SH and AC are indicated by subscripts. Heating loads are shown as positive values and the AC loads are shown as negative values. Error bars for the loads indicate the range of values recorded for that particular hour. The hourly-averaged loads are investigated over 24-hours during summer, winter and nominal periods of the year, which definitions are explained in Sections 4.1. Fig. 5D shows the annual heating and AC cooling energy supplied by the R744 system, *E*, and ambient temperatures on a monthly basis. The hourly-averaged loads and the monthly total energy consumption are used to evaluate the performance of the system for the full range of operation from September 2018 to September 2019. The trends for the different loads are discussed individually in the following paragraphs. It should also be stated that the Y-axis temperature scale for the seasonal cases are different.

- $\dot{Q}_{SH}$: The SH load is dependent on $T_{a,\ avg}$ and varies in a range of 5–100 kW for the different seasonal scenarios displayed in Fig. 5A–C. The lowest recorded values are observed in the summer case, where $\dot{Q}_{SH}$ decreases significantly when $T_{a,\ avg}$ exceeds 15 °C. In this case, the entirety of $\dot{Q}_{SH}$ is supplied to the batteries in the ventilation units. Naturally, the highest recorded hourly-averaged values are observed in the winter scenario in Fig. 5B. Approximately 80% of $\dot{Q}_{SH}$ is then supplied to the ventilation units, due to the relatively large capacity of these units. Thus, only a small portion of the heat load is used to cover direct SH, e.g. for floor heating and radiators.

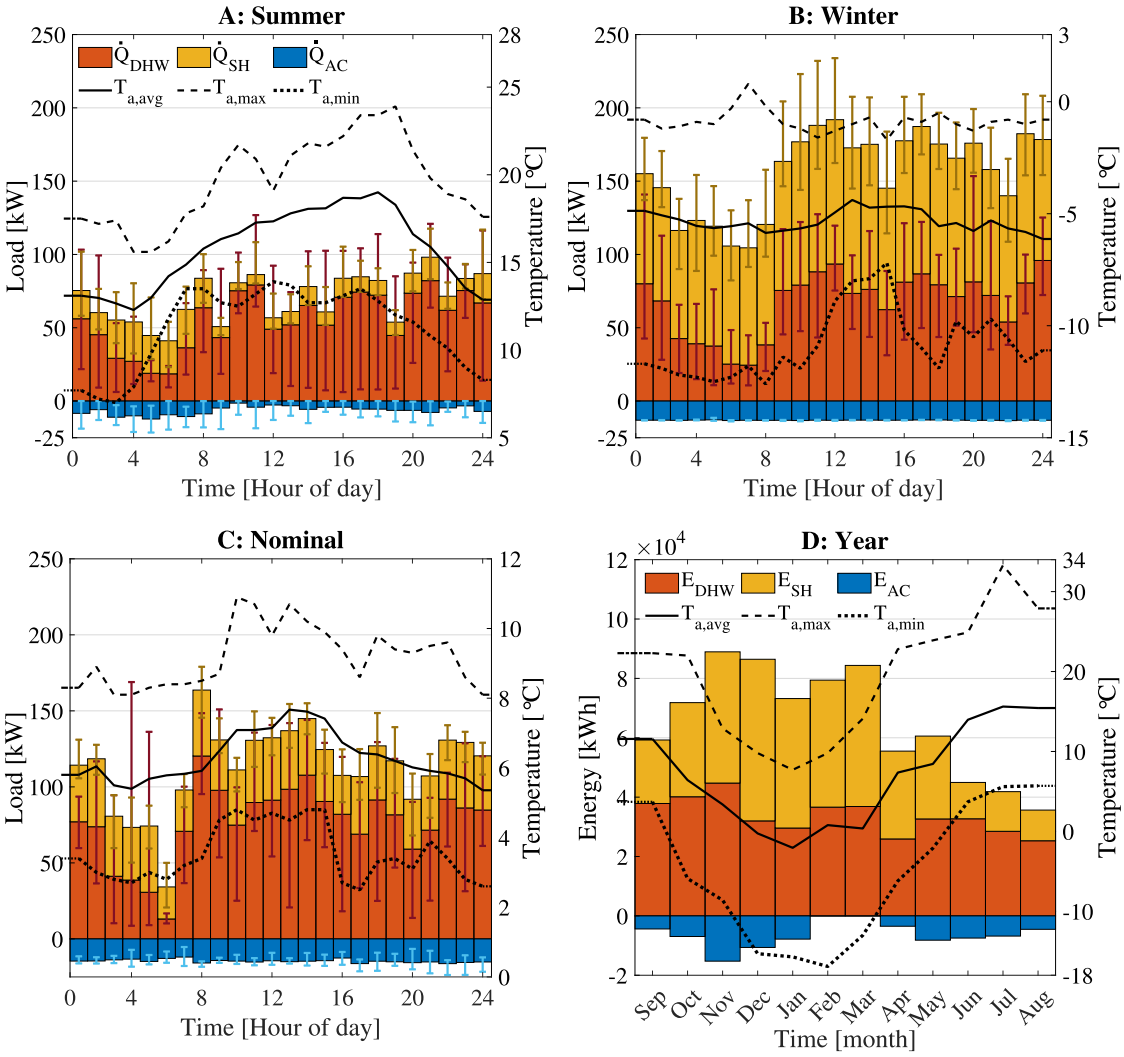

Fig. 5. Hourly-averaged heating and AC loads for (A) summer (May 18th–25th 2019), (B) winter (January 15th to 22nd 2019) and (C) nominal (October 18th–25th 2018). Total annual energy supplied by the R744 unit on (D) monthly basis (Sep. 2018 to Sep. 2019).

- $\dot{Q}_{DHW}$: The DHW loads in Fig. 5A to 5 C drop to the minimum value of 20 to 30 kW at hour 6, followed by a rapid increase in $\dot{Q}_{DHW}$ between 60 to 80 kW, which stay present throughout the day. A noticeable difference in the magnitude of $\dot{Q}_{DHW}$ is shown in the various seasonal scenarios. These inconsistencies are due to variations in guest load and are independent of seasonal operational load and $T_{a,\,avg}$.
- $\dot{Q}_{AC}$: The AC refrigeration capacity varies in a limited range of 0 to 24 kW in all seasonal cases. The load is independent of the hour-of-day and $T_{a,\,avg}$. However, the AC load provided by the R744 is not independent of $T_{a,\,avg}$. This unusual behavior in supplied AC load from the R744 unit is caused by the fact that it is an auxiliary system to the pre-installed separate cooling unit. It should be noted that AC cooling provided by the primary stand-alone chiller is not included in Fig. 5A–D. The separate AC chiller unit is operating at full load during the summer scenario in Fig. 5A, though hardly any AC is supplied by the R744 unit during this time due to the low-side pressure control. As shown in Fig. 1, the air evaporators and HX6 in the R744 unit operate at the same pressure level, controlled solely by the air evaporators. The R744 unit therefore only supplies extra AC when the evaporation temperature is below the 7 °C setpoint for AC chilled water. The largest $\dot{Q}_{AC}$ capacities are observed in the winter and nominal scenarios in Fig. 5B and C, respectively. In these scenarios, moderate $T_{a,\,avg}$ enables operation of the chilled water HX within the acceptable evaporation-temperature range.
- E_{SH}: E_{SH} varies in a range of approximately 10,000 to 55,000 kWh, in close connection to $T_{a,\,avg}$. As shown in Fig. 5D, the heating demand is still present during the summer months, due to the relatively cold climate at the hotel's location. The largest recorded values of E_{SH} is observed during the winter months when $T_{a,\,avg}$ is below 5 °C. E_{SH} is then in a range of 42,000–55,000 kWh monthly, which is up to 5 times the SH usage for the summer months. The total amount of E_{SH} over the year is 380,000 kWh.
- E_{DHW}: The monthly energy for DHW shown in Fig. 5D is stable throughout the year in a range of 30,000 to 40,000 kWh per month, with an average value of 33,600 kWh. The annual energy supplied for DHW over the year is 403,000 kWh. Thus, 52% of the annual heating energy to the hotel is allocated to DHW heating. The relative consumption of DHW to total heating in hotels is typically between 40 and 70%,

Table 1
COPs for selected intervals in the period from Sep. 2018 to Sep. 2019.

Season	Period	$SCOP_{sys}$[-]	$SCOP_{sys+el}$[-]	$SCOP_h$[-]	$T_{a,\,avg}$[°C]
Winter	November–April	2.78 ± 0.17	2.57 ± 0.27	2.69 ± 0.15	0.4
	January 15th to 22nd	2.63 ± 0.16	2.37 ± 0.25	2.49 ± 0.14	−5.3
Summer	June–September	3.20 ± 0.20	2.75 ± 0.29	3.09 ± 0.18	15.0
	May 18th–25th	3.34 ± 0.21	2.97 ± 0.31	3.30 ± 0.19	15.8
Nominal	September–November, April–June	2.99 ± 0.19	2.73 ± 0.29	2.90 ± 0.17	8.4
	October 18th–25th	3.23 ± 0.20	3.21 ± 0.34	3.05 ± 0.17	6.3
Annual	September–September	2.90 ± 0.18	2.64 ± 0.28	2.80 ± 0.16	6.8

Seasonal intervals are from the 1*st* to the 1*st* in the stated months.

and is dependent on the location, building envelope and use of facilities (Su, 2012; Deng and Burnett, 2000).

– E_{AC}: As previously explained, E_{AC} is larger during the nominal months of operation. AC is primarily used for climate control and temperature adjustments in common areas and guest rooms. The AC cooling capacity is therefore larger during periods with high guest loads and large heating demands. For the entire year, only 75,500 kWh of AC cooling energy was recovered through the chilled water HX.

4.2.2. Coefficient of performance (COPs)

The SCOPs for the scenarios depicted in Fig. 5, together with seasonal and annual values are listed in Table 1. The average ambient temperature, $T_{a,\,avg}$, for the specified intervals are included in the table. Predictably, $SCOP_{sys}$ is higher than $SCOP_h$ for the investigated scenarios. However, the annual $SCOP_{sys}$ is only 0.1 or 3.6% higher than the $SCOP_h$. Byrne et al. (2009) estimated numerically a SCOP of 3.57 for a heat pump and chiller system for hotels using R407a. They also investigated an R744 system with similar operational conditions and found a SCOP of 3.24. However, secondary systems and real operating conditions were not accounted for in this study. The conventional thermal systems found in the Nordic hotel market normally utilize electric boilers/district heating stations in combination with separate HFC-units for AC. Typically, a $SCOP_{sys}$ in the vicinity of 1 is achieved for these systems, due to the relatively large magnitude of heating load to AC load. The somewhat low value of annual $SCOP_{sys}$ for the integrated system is partially due to the limited recovery of cold energy to the AC cooling circuit. This is also the case for the long-term seasonal periods, e.g. winter, summer and nominal. On an annual basis, approximately 5% of the total heat to the hotel is supplied by the electric boiler. As a result, $SCOP_{sys+el}$ is reduced by 9% when compared to $SCOP_{sys}$. It is expected that the boiler is applied during the winter season to cover peak heating. However, the low value of $SCOP_{sys+el}$ during the summer season indicates excessive use of the boiler for DHW heating. This is explained by the high return temperature of water to GC2. A temperature above 45 °C triggers a signal to reduce the compressor capacity, due to compromised efficiency. Consequently, DHW production by the heat pump is reduced and the required load is then compensated by the boiler.

All SCOPs are highly dependent on $T_{a,\,avg}$ and increase with approximately 0.4 from the winter to the summer season. A larger difference between the specific SCOPs is observed when comparing the summer and winter week scenarios (Fig. 5A and B), which can be attributed to the change in $T_{a,\,avg}$. The nominal week of October 18th–25th reveals uncharacteristically high values of $SCOP_{sys}$ when related to the nominal season. Moreover, $T_{a,\,avg}$ for this week is 2.1 °C below the average temperature for the particular season. The high value of $SCOP_{sys}$ during this week can be explained by the relatively large utilization of AC, as displayed in Fig. 5C. The gain from $\dot{Q}_{AC}$ is therefore larger than the contribution from $\dot{W}_{fan}$ and $\dot{W}_{aux,el}$ in the calculation of $SCOP_{sys}$, as defined in Eq. (8).

The mean COP_{sys} and COP_h for transcritical operations (> 73.9 bar), according to specific temperature intervals, are listed in Table 2. The COPs are categorized by whether or not DHW charging is taking place. The subscript *nch* includes circumstances when the heat supply to the hotel is controlled by SH demands, and no active charging of the DHW storage is taking place. Situations when the DHW storage is being actively charged, and the system is controlled according to both SH and DHW loads are identified by the subscript *ch*. The analysis of variance (ANOVA: single factor) was applied to analyze the efficiency of the system under different modes of operations. The difference is considered significant at $p < 0.05$.

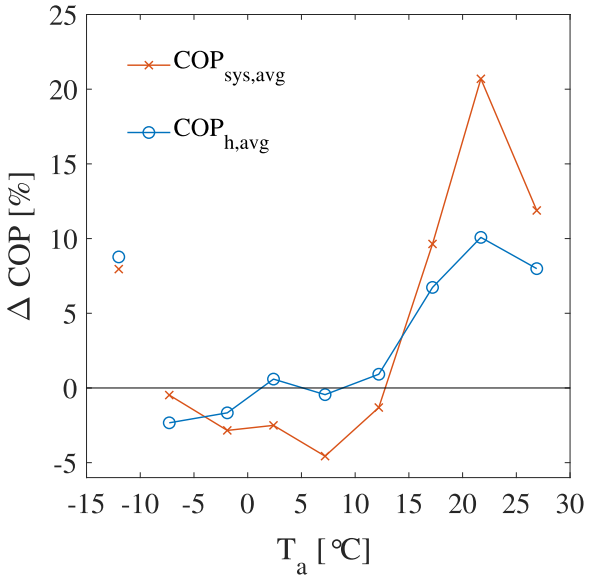

Fig. 6. Difference between the DHW charging and no charging COPs.

Table 2 shows a significant difference between charging and no charging values of $COP_{h,\,avg}$ at temperatures below 0 °C and above 15 °C. $COP_{sys,\,avg}$ exhibit significant difference between all intervals, with the exception of −10 to −5 °C and 10 to 15 °C. Fig. 6 depicts the relative change in COP, ΔCOP [%], from no charging (COP_{nch}) to charging (COP_{ch}). The COPs during no DHW charging are generally higher than charging mode at low temperatures, which results in a decrease of ΔCOP. However, both $COP_{sys,\,avg}$ and $COP_{h,\,avg}$ increase considerably at T_a above 15 °C. This unusual relationship between the two modes of operation can be explained by the magnitude of the SH load and the temperature of the water returning to the second gas cooler. The temperature of the fluid returning from the secondary system is generally higher at high values of SH, as the setpoints of SH and thus the return temperatures are elevated at low values of T_a. Additionally, DHW charging provides a temperature lift in the return circuit when the stratification in the DHW storage is not fully intact, as discussed in Sections 4.1.2. This behavior was also illustrated by Tosato et al. (2019). They noted a reduction in COP of 18% during the final part of the DHW charging process, which was caused by high return temperatures from the

Table 2
System and heating COPs during DHW charging and no charging at different temperature intervals.

T_a [°C]	[−15,−10)	[−10,−5)	[−5,0)	[0,5)	[5,10)	[10,15)	[15,20)	[20,25)	[25,30)
$\mathbf{COP}_{sys\,ch,\,avg}$ [−]	2.59 (0.50)	2.40[a] (0.22)	2.53 (0.34)	2.82 (0.44)	3.17 (0.50)	3.38[a] (0.58)	3.37 (0.61)	3.38 (0.62)	3.28 (0.50)
$\mathbf{COP}_{sys\,nch,\,avg}$ [−]	2.40 (0.70)	2.41[a] (0.33)	2.61 (0.56)	2.89 (0.66)	3.32 (0.68)	3.43[a] (0.92)	3.07 (0.92)	2.80 (0.83)	2.93 (0.85)
$\mathbf{COP}_{h\,ch,\,avg}$ [−]	2.47 (0.46)	2.32 (0.23)	2.53 (0.34)	2.77[a] (0.45)	3.03[a] (0.47)	3.11[a] (0.50)	3.19 (0.54)	3.23 (0.57)	3.24[a] (0.53)
$\mathbf{COP}_{h\,nch,\,avg}$ [−]	2.27 (0.70)	2.38 (0.31)	2.58 (0.49)	2.76[a] (0.57)	3.04[a] (0.53)	3.08[a] (0.80)	2.99 (0.87)	2.93 (0.87)	3.00[a] (0.85)
$\mathbf{T}_{a\,ch,\,avg}$ [°C]	−12.0 (1.3)	−7.2 (1.4)	−2.0 (1.4)	2.4 (1.5)	7.4 (1.4)	12.3 (1.4)	17.3 (1.5)	21.9 (1.3)	26.9 (1.4)
$\mathbf{T}_{a\,nch,\,avg}$ [°C]	−12.1 (1.3)	−7.5 (1.4)	−1.8 (1.4)	2.3 (1.4)	7.1 (1.5)	12.0 (1.4)	17.0 (1.5)	21.6 (1.3)	26.8 (1.4)

[a] No significant statistical difference ($p > 0.05$) between corresponding DHW charging and no charging values. Standard deviation is shown in the brackets. Values for calculated measurement uncertainties are not included.

storage. Hence, during seasons with low T_a, high SH and thus generally high return fluid temperature, the heating load of the CO_2 unit is limited due to high $T_{gc,exit}$. This problem diminishes when the SH load is limited, as can be observed in Fig. 6 at T_a above 15 °C. The COPs during DHW charging are generally higher than the no charging mode at high ambient temperatures, which is in agreement with the findings in Tosato et al. (2019). Thus, the DHW charging strategy of the system should be regarded as a key influencing factor to achieve high efficiency.

5. Conclusions

This work investigated key operating parameters for an R744 heating and AC cooling unit installed in a Norwegian hotel. The system is integrated with HVAC, DHW and a 6 m^3 thermal storage. Field measurements from the hotel were analyzed for a one-year period and essential parameters to evaluate the system performance were discussed, including heating and AC loads, temperatures, pressures and mass flow rates. DHW consumption loads and COPs were calculated using the collected data. The DHW consumption was estimated by the energy balance due to the peculiarities of the instrumentation installed by the supplier. Consequently, the heat loss from the storage tanks were included in the DHW consumption rate and thus not evaluated in this study. The same applies to the existing AC cooling machine, as this unit is not integrated in the measurement and control system.

The heating and AC loads supplied by the R744 unit were studied on a weekly and monthly basis to assess the seasonal behavior of the system. The results reveal that the DHW load is fairly stable throughout the year and is independent of seasonal ambient temperatures. The DHW load accounts for 52% of the annual heat load supplied to the hotel and follows a particular 24-h pattern, with low consumption between midnight and hour 6. The peak DHW load occurs around hour 9 and reaches an hourly-averaged value of 73 kWh. The DHW storage holds an energy capacity of 350 kWh at fully charged conditions and demonstrates peak demand compensation of more than 100 kW during October 18th–20th 2018. Periodical decrease in storage temperatures to values below the set-point indicates that the storage is not fully equipped to handle the peak DHW loads of the hotel. This can be solved by installing more tanks in series or by increasing the water storage temperature.

The COPs during DHW charging mode are higher when compared with no charging at ambient temperatures above 15 °C, due to limited SH demands. The SH is highly dependent on ambient temperatures and varies noticeably in the different seasonal scenarios. The monthly supply of SH energy increases significantly at average ambient temperatures below 5 °C. The AC capacity delivered by the R744 unit is limited and not fully exploited, which is reflected in the moderate annual $SCOP_{sys}$ of 2.90. Additionally, about 5% of the total heat to the hotel is supplied by the electric boiler, which decreases overall $SCOP_{sys}$ by 9%. The latter is often a result of high return temperatures from the building, which is aggravated by increased number of R744 unit starts and stops and mixing in DHW tanks. Other factors that greatly influence the efficiency of the system are variations in the ambient temperatures and high temperatures at the gas cooler exit.

Observations from this work can be used as a good starting point for modeling and optimization of the existing and similar systems. Future work should focus on increasing the system performance by charging the storage during longer periods at reduced capacities. The optimal storage volume for this type of system is an important issue that should be prioritized.

Declaration of Competing Interest

The authors declare that they have no known competing financial interests or personal relationships that could have appeared to influence the work reported in this paper.

Acknowledgments

The authors would like to acknowledge the Norwegian Research Council for funding this project. We would also like to thank Kelvin AS for in-depth system details and Scandic Hotel Hell for access to their system data. Also, we would like to acknowledge Yannick Pruss for his contribution to this research work.

Supplementary material

Supplementary material associated with this article can be found, in the online version, at doi:10.1016/j.ijrefrig.2020.03.021.

References

Bamigbetan, O., Eikevik, T.M., Nekså, P., Bantle, M., 2017. Review of vapour compression heat pumps for high temperature heating using natural working fluids. Int. J. Refrig. 80, 197–211.
Bohdanowicz, P., 2006. Responsible Resource Management in Hotels: Attitudes, Indicators, Tools and Strategies. KTH.
Bolaji, B., Huan, Z., 2013. Ozone depletion and global warming: case for the use of natural refrigerant–a review. Renew. Sustain. Energy Rev. 18, 49–54.
Byrne, P., Miriel, J., Lenat, Y., 2009. Design and simulation of a heat pump for simultaneous heating and cooling using HFC or CO_2 as a working fluid. Int. J. Refrig. 32 (7), 1711–1723.
Cecchinato, L., Corradi, M., Cosi, G., Minetto, S., Rampazzo, M., 2012. A real-time algorithm for the determination of R744 systems optimal high pressure. Int. J. Refrig. 35 (4), 817–826.
Cecchinato, L., Corradi, M., Fornasieri, E., Zamboni, L., 2005. Carbon dioxide as refrigerant for tap water heat pumps: a comparison with the traditional solution. Int. J. Refrig. 28 (8), 1250–1258.
Cecchinato, L., Corradi, M., Minetto, S., 2010. A critical approach to the determination of optimal heat rejection pressure in transcritical systems. Appl. Therm. Eng. 30 (13), 1812–1823.
Chua, K.J., Chou, S.K., Yang, W., 2010. Advances in heat pump systems: a review. Appl. Energy 87 (12), 3611–3624.
Ciconkov, R., 2018. Refrigerants: there is still no vision for sustainable solutions. Int. J. Refrig. 86, 441–448.
Council of the European Commission and others (EC), 2010. Directive 2010/31/EU of the European Parliament and of the council of 19 May 2010 on the energy performance of buildings. Off. J. Eur. Union L 153, 13–35.
D'Agaro, P., Coppola, M., Cortella, G., 2019. Field tests, model validation and performance of a CO_2 commercial refrigeration plant integrated with HVAC system. Int. J. Refrig. 100, 380–391.
Dalton, G., Lockington, D., Baldock, T., 2008. Feasibility analysis of stand-alone renewable energy supply options for a large hotel. Renew. Energy 33 (7), 1475–1490.

Danfoss, 2012. Application guide: 1 and 2 stage Transcritical CO_2 systems – how to control the system. Application guide RA8AA302 http://files.danfoss.com/TechnicalInfo/Dila/01/RA8AA302.pdf.

Danfoss, 2015. Application guide: heat reclaim in transcritical CO_2systems. Application guide DKRCE.PA.R1.F1.22 https://assets.danfoss.com/documents/DOC167786419094/DOC167786419094.pdf.

Deng, S.-M., Burnett, J., 2000. A study of energy performance of hotel buildings in Hong Kong. Energy Build. 31 (1), 7–12.

Deng, S.-M., Burnett, J., 2002. Water use in hotels in Hong Kong. Int. J. Hosp. Manag. 21 (1), 57–66.

Economidou, M., Atanasiu, B., Despret, C., Maio, J., Nolte, I., Rapf, O., 2011. Europe's Buildings Under the Microscope. aCountry-by-Country Review of the Energy Performance of Buildings. Buildings Performance Institute Europe (BPIE), pp. 35–36.

European Commission (EC), 2006. Action Plan for Energy Efficiency: realising the potential, communication from the commission, COM (2006) 545 Final. https://eur-lex.europa.eu/legal-content/EN/TXT/PDF/?uri=CELEX:52006DC0545&from=EN

European Parliament and Council of the European Union (EP and EC), 2014. Eu regulation no 517/2014 of the european parliament and of the council of 16 april 2014 on fluorinated greenhouse gases and repealing regulation (EC) no 842/2006. Official J. Eur. Union 57, 195–230.

Eurostat, 2017. Final energy consumption by sector. Accessed: 2019-11-11 https://ec.europa.eu/eurostat/databrowser/view/ten00124/default/table?lang=en.

Fabrizio, E., Seguro, F., Filippi, M., 2014. Integrated HVAC and DHW production systems for Zero Energy Buildings. Renew. Sustain. Energy Rev. 40, 515–541.

Fernandez, N., Hwang, Y., Radermacher, R., 2010. Comparison of CO_2 heat pump water heater performance with baseline cycle and two high COP cycles. Int. J. Refrig. 33 (3), 635–644.

Girotto, S., 2016. Direct Space Heating and Cooling with CO_2Refrigerant. ATMOsphere Europe.

Gullo, P., 2019. Innovative fully integrated transcritical R744 refrigeration systems for a HFC-free future of supermarkets in warm and hot climates. Int. J. Refrig. 108, 283–310.

Gullo, P., Elmegaard, B., Cortella, G., 2016. Advanced energy analysis of a R744 booster refrigeration system with parallel compression. Energy 107, 562–571.

Gullo, P., Hafner, A., Banasiak, K., 2018. Transcritical R744 refrigeration systems for supermarket applications: current status and future perspectives. Int. J. Refrig. 93, 269–310.

Gullo, P., Hafner, A., Banasiak, K., 2019. Thermodynamic performance investigation of commercial R744 booster refrigeration plants based on advanced exergy analysis. Energies 12 (3), 354.

Hafner, A., 2015. 2020 perspectives CO_2 refrigeration and heat pump systems. In: Proceedings of the 6th IIR Ammonia and CO_2 Refrigeration Technologies Conference, Ohrid, Macedonia, pp. 16–18.

Hafner, A., 2017. Integrated CO_2 system refrigeration, air conditioning and sanitary hot water. In: Proceedings of the 7th IIR Ammonia and CO_2 Refrigeration Technologies Conference, Ohrid, Macedonia, pp. 11–13.

Heinz, A., Martin, K., Rieberer, R., Kotenko, O., 2010. Experimental analysis and simulation of an integrated CO_2 heat pump for low-heating-energy buildings. In: 9th IIR Gustav Lorentzen Conference 2010. ..

Hotel Energy Solutions (HES), 2011. Analysis on energy use by European hotels: Online survey and desk research. http://hes.unwto.org/sites/all/files/docpdf/analysisonenergyusebyeuropeanhotelsonlinesurveyanddeskresearch2382011-1.pdf

Hu, B., Li, Y., Cao, F., Xing, Z., 2015. Extremum seeking control of COP optimization for air-source transcritical CO_2 heat pump water heater system. Appl. Energy 147, 361–372.

IWMAC, 2019. Centralized operation and surveillance by use of WEB technology. https://www.iwmac.com/

Karampour, M., Sawalha, S., 2017. Energy efficiency evaluation of integrated CO_2 trans-critical system in supermarkets: a field measurements and modelling analysis. Int. J. Refrig. 82, 470–486.

Lawson F., 2001. Hotels and Resorts – Planning, Design and Refurbishment Architectural Press; London, UK (2001).

Liu, S., Li, Z., Dai, B., 2017. Energy, economic and environmental analyses of the CO_2heat pump system compared with boiler heating system in China. Energy Procedia 105, 3895–3902.

Lorentzen, G., 1994. Revival of carbon dioxide as a refrigerant. Int. J. Refrig. 17 (5), 292–301.

Minetto, S., 2011. Theoretical and experimental analysis of a CO_2 heat pump for domestic hot water. Int. J. Refrig. 34 (3), 742–751.

Minetto, S., Cecchinato, L., Brignoli, R., Marinetti, S., Rossetti, A., 2016. Water-side reversible CO_2 heat pump for residential application. Int. J. Refrig. 63, 237–250.

Ndoye, B., Sarr, M., 2008. Analysis of domestic hot water energy consumption in large buildings under standard conditions in Senegal. Build. Environ. 43 (7), 1216–1224.

Nekså, P., 2002. CO_2 heat pump systems. Int. J. Refrig. 25 (4), 421–427.

Nekså, P., Rekstad, H., Zakeri, G.R., Schiefloe, P.A., 1998. CO_2-heat pump water heater: characteristics, system design and experimental results. Int. J. Refrig. 21 (3), 172–179.

Nekså, P., Walnum, H.T., Hafner, A., 2010. CO_2– a refrigerant from the past with prospects of being one of the main refrigerants in the future. In: 9th IIR Gustav Lorentzen Conference. Citeseer, pp. 2–14.

Omer, A.M., 2008. Ground-source heat pumps systems and applications. Renew. Sustain. Energy Rev. 12 (2), 344–371.

Pardiñas, Á.Á., Hafner, A., Banasiak, K., 2018. Novel integrated CO_2 vapour compression racks for supermarkets. thermodynamic analysis of possible system configurations and influence of operational conditions. Appl. Therm. Eng. 131, 1008–1025.

Polzot, A., D'Agaro, P., Gullo, P., Cortella, G., 2016. Modelling commercial refrigeration systems coupled with water storage to improve energy efficiency and perform heat recovery. Int. J. Refrig. 69, 313–323.

Rankin, R., Rousseau, P., 2006. Sanitary hot water consumption patterns in commercial and industrial sectors in South Africa: impact on heating system design. Energy Convers. Manag. 47 (6), 687–701.

Santamouris, M., Balaras, C., Dascalaki, E., Argiriou, A., Gaglia, A., 1996. Energy conservation and retrofitting potential in Hellenic hotels. Energy Build. 24 (1), 65–75.

Sarkar, J., Bhattacharyya, S., Gopal, M.R., 2004. Optimization of a transcritical CO_2 heat pump cycle for simultaneous cooling and heating applications. Int. J. Refrig. 27 (8), 830–838.

Sarkar, J., Bhattacharyya, S., Gopal, M.R., 2006. Simulation of a transcritical CO_2 heat pump cycle for simultaneous cooling and heating applications. Int. J. Refrig. 29 (5), 735–743.

Shecco, 2016. Guide 2016: Guide to Natural Refrigerants in Japan -State of the Industry. Brussel, Belgium.

Skačanová, K.Z., De Oña, A., 2019. Market and technology trends for CO_2 and Ammonia in commercial and industrial refrigeration. In: Proceedings of the 8th IIR Ammonia and CO_2 Refrigeration Technologies Conference, Ohrid, Macedonia, pp. 334–338.

Skaugen, T., Tveito, O., Førland, E., 2002. Heating Degree-Days – Present Conditions and Scenario for the Period 2021–2050. DNMI report.

Smitt, S., Hafner, A., Hoksrød, E., 2019. Presentation of the first combined CO_2 heat pump, air conditioning and hot tap water system for a hotel in Scandinavia. In: Proceedings of the 8th Conference on Ammonia and CO_2 Refrigeration Technologies. 11-13 April 2019. Ohrid, Republic of Macedonia

Stene, J., 2005. Residential CO_2 heat pump system for combined space heating and hot water heating. Int. J. Refrig. 28 (8), 1259–1265.

Su, B., 2012. Hotel design and energy consumption. World Acad. Sci. Eng. Technol. 72, 1655–1660.

Tammaro, M., Mauro, A., Montagud, C., Corberán, J., Mastrullo, R., 2016. Hot sanitary water production with CO_2 heat pumps: effect of control strategy on system performance and stratification inside the storage tank. Appl. Therm. Eng. 101, 730–740.

Thom, H., 1954. The rational relationship between heating degree days and temperature. Mon. Weather Rev. 82 (1), 1–6.

Tosato, G., Girotto, S., Minetto, S., Rossetti, A., Marinetti, S., 2019. An integrated CO_2 unit for heating, cooling and DHW installed in a hotel. Data from the field.. In: 37th UIT Heat Transfer Conference.

United Nations Environment Programme (UNEP), 2016. Decision XXVIII/Further Amendment of the Montreal Protocol. Twenty-Eighth Meeting of the Parties to the Montreal Protocol on Substances That Deplete the Ozone Layer. UNEP/OzL.Pro.28/CRP/10, United Nations Environment Programme, Nairobi, Kenya, 14 October.

Wang, S., Tuo, H., Cao, F., Xing, Z., 2013. Experimental investigation on air-source transcritical CO_2 heat pump water heater system at a fixed water inlet temperature. Int. J. Refrig. 36 (3), 701–716.

Yang, L., Li, H., Cai, S.-W., Shao, L.-L., Zhang, C.-L., 2015. Minimizing COP loss from optimal high pressure correlation for transcritical CO_2 cycle. Appl. Therm. Eng. 89, 656–662.

Yokoyama, R., Shimizu, T., Ito, K., Takemura, K., 2007. Influence of ambient temperatures on performance of a CO_2 heat pump water heating system. Energy 32 (4), 388–398.